

Trends in pK_a Values for polyprotic carboxylic acids

Shivam Parashar and Prateek Kumar Jha*

Department of Chemical Engineering, Indian Institute of Technology Roorkee

E-mail: pkjchfch@iitr.ac.in

Abstract

In this work we have reported the pK_a values for straight chain (without branches) oligomers of Acrylic acid using CBS-QB3 gas phase energies with solvation free energies from CPCM/HF 6-31G(d) and SMD/B3LYP (2df,p). We have found that the negative log of the first acid dissociation constant decreases with the chain length. Within a chain, the microscopic pK_a for the COOH groups present at the end of the chain is maximum and minimum for centrally located COOH groups.

Introduction

A lot of research has been conducted to model and predict the pK_a values for small inorganic acids using quantum mechanics.¹ Effect of thermodynamic cycle,² model chemistries,² implicit and explicit solvation² and solute cavity³ on the accuracy of the pK_a values has also been investigated. There has been fewer studies³⁻⁵ for investigation of acidity constants for polymeric acids because of presence of multiple acid groups. These acids have a range of applications in specific bioseparation and catalysis.⁶ In this study we have considered the oligomers of acrylic acid, in which a single kind of functional group (COOH) is present, and the microscopic pK_a value of each site is dependent on its location relative to the molecule. In case of a protein, the same -COOH group could have a pK_a value of 2 and 9 units⁷ indicating the significance of the electrostatic environment.

The high-level ab initio CBS-QB3 and CBS-APNO methods (using HF 6-31 G(d) and HF 6-31+ G(d)) with CPCM generated smallest inaccuracy of about 0.5 log unit when

commonly used, and the simplest thermodynamic cycle (without involving water molecule) was employed.⁸

Qian et al.⁵ have reported the pK_a values for different conformers for dimer and trimer of methacrylic acid. They found the pK_a values of the oligomers to be greater than the monomer. But they had not considered the anionic structures in which intramolecular H-bonding could stabilize the structure thereby facilitating easy acid dissociation.

Theory

The Continuum solvent models⁹ have been parametrized to give accurate solvation energies at low levels of theory. The accuracy of continuum solvent calculations of aqueous pK_a s lies in the range of 2-3 units.¹⁰ For accurately calculating the free energy in the solvent, the solvation energy should be combined with the high-level ab initio methods for the gas-phase which is accomplished by using an appropriate thermodynamic cycle. We have used a Direct thermodynamic cycle to compute ΔG_{aq} . The direct cycle has provided errors of approximately 0.5 pK_a units or lower for carboxylic acids.⁸ ΔG_{aq} is given by -

$$\Delta G_{aq} = \Delta G_{gas} + \Delta\Delta G_{sol} \quad (1)$$

Where ΔG_{gas} is given by -

$$\Delta G_{gas} = G_{gas}(H^+) + G_{gas}(A^-) - G_{gas}(HA) \quad (2)$$

and $\Delta\Delta G_{sol}$ can be written as -

$$\Delta\Delta G_{sol} = \Delta G_{sol}(H^+) + \Delta G_{sol}(A^-) - \Delta G_{sol}(HA) \quad (3)$$

All the terms in RHS of equation 2 and 3 were computed except $G_{gas}(H^+)$ and $\Delta G_{sol}(H^+)$ as free energy cannot be calculated for a proton since it does not contain any electrons. Therefore, those values were taken from experiments.

After assuming that the thermal contributions are similar in both the gas and solution phase, each term of ΔG_{sol} in equation 3 was calculated as¹¹ -

$$\Delta G_{sol} = (E_{soln} + G_{nes}) - E_{gas} \quad (4)$$

where E_{soln} and E_{gas} are the electronic energy of molecule in presence and absence of

the solvent field respectively. G_{nes} is the sum of all non-electrostatic contributions which includes cavitation and dispersion-repulsion terms. In Gaussian 09, the single point energy obtained using SMD solvent phase calculations contains the non-electrostatic terms in itself. Therefore, solvation energy using SMD model is simply computed as the difference between electronic energy on solution-phase and gas-phase optimized geometries.

For acidic sites present in an oligomer of acrylic acid, the dissociation of the proton from each site cannot be assumed to be stepwise. This case is dissimilar to the classic treatment of a polyprotic acid, for which difference in successive pKa is large enough to ignore the second or third deprotonation. The equilibrium dissociation constants of individual acidic groups are referred to as microscopic dissociation constants. Their relation to macroscopic dissociation constant, which represents the ability of the whole molecule to lose a proton is given by -

$$K_1 = k_x + k_y \tag{5}$$

where k_x and k_y are the microscopic dissociation constant for acidic sites x and y respectively in a dimer of polyprotic acid, and K_1 is the first macroscopic dissociation constant for the dimer.

Simulations

All simulations were performed on Gaussian 09¹² program. Starting geometries for anions were prepared by deleting the appropriate hydrogen atom from their corresponding protonated forms. Several starting geometries were taken and only the most stable conformation energies are reported. It was assumed that the most stable conformer was the one with the least single point energy. Since for each oligomer, there are multiple possible low lying conformers, we optimized the molecule with different starting structures.

A frequency calculation was also done after the optimization to insure that the no imaginary frequencies are there and the structure is optimized to a true minimum state. In case the high level hessian matrix did not optimized the structure to a true minima, the structure was reoptimized taking the previous unoptimized structure as its initial guess.

The SMD model has been parametrized with a training set of 2821 solvation data including 112 aqueous ionic solvation free energies, 220 solvation free energies for 166 ions in acetonitrile, methanol, and dimethyl sulfoxide, 2346 solvation free energies for 318 neutral solutes in 91 solvents (90 nonaqueous organic solvents and water), and 143 transfer free energies for 93 neutral solutes between water and 15 organic solvents.¹³

Gas-phase energy Calculation

There are a bunch of methods available in gaussian for calculating accurate gas phase energies. Some of them are G1, G2, G3, G4, G2(MP2), G3(MP2) etc. All these methods involve doing several predefined calculations for energy computation. CBS-QB3 is equally accurate and computationally efficient than the above methods.

We have used CBS-QB3¹⁴ model chemistry to compute ΔG_{gas} values. It produces mean absolute deviations of 1.43 pka units¹⁵ for small molecules. CCSD(T) calculations are most accurate and they can give gas-phase free energies as close to the experimental values. But because of their huge computational time, its application is limited to smaller molecules only. CBS-QB3 makes use of optimized geometry from density functional theory and then Single point calculations are performed at various levels such as CCSD(T), MP4SDQ, and MP2.¹

Solvation energy Calculation

In an earlier study by Liptak and Shields, the authors showed that calculations using continuum models on the lowest energy gas-phase conformer and the conformationally averaged structure gave comparable results¹ Accordingly, in this study we only consider the solvation free energies on the lowest energy gas-phase conformer. We have used implicit solvent model in which the solvent is represented as a polarizable dielectric continuum. Explicit treatment of solvent molecules would be extremely expensive for larger molecule that we are dealing here with. The conductor-polarizable continuum model (CPCM)¹⁶ was used to compute solvation free energies at the HF/6-31 G(d) and SMD was used alongside with B3LYP/6-31 G(2df,p). All geometries of the studied species have been optimized fully in the presence of solvent and their respective level of theories. The implicit model is computationally less expensive than explicit solvent as it approximates the response of the bulk solvent using a homogeneous dielectric continuum. Implicit model does not provides accurate solvation energies for anionic structures because it does not takes into account individual solute-solvent interaction. However, it performs well for neutral species. In Gaussian 09 the default option is Radii=UA0 (Topological United Atoms model) which treats functional groups as a single sphere. We have optimized the geometry at gas phase and solution phase as well because it increases the accuracy of the pKa values.¹⁷ Solvation energy was computed as the difference between single point energy in solution phase and in gas phase.

Results

Table 1: Summary of the gas-phase and solvation energies for oligomers of Acrylic acid.

Molecule	ΔG_{gas} CBS-QB3 (kcal/mol)	ΔG_{sol} (kcal/mol)				Relative pK_a	
		HF/6-31G(d)//CPCM		B3LYP/6-31G(2df,p)//SMD		HF	B3LYP
		Anion	Acid	Anion	Acid		
Propanoic acid	345.68	-65.88	-5.02	-71.20	-4.97	4.87*	4.87*
Dimer(Anion-1)	324.447	-57.21	-9.75	-58.70	-11.34	-0.87	3.14
Dimer(Anion-3)	324.452	-56.55	-9.75	-58.03	-11.34	-0.39	3.63
Trimer(Anion-1)	322.41	-59.63	-13.99	-62.25	-17.99	-1.03	3.91
Trimer(Anion-3)	313.41	-53.02	-13.99	-52.29	-17.99	-2.79	4.62
Trimer(Anion-5)	322.91	-58.73	-13.99	-60.40	-17.99	0.00	5.64

Table 1 summarizes the gas-phase, solvation free energies and pka values for the oligomers of Acrylic acid. Figure 1 and figure 2 shows the optimized structures of dimer, trimer and their conjugate base structures obtained from CBS-QB3 gas phase calculations. Optimizing the geometry by other methods such as DFT/B3LYP(2df,p) and HF/6-31G(d) in gas phases and using SMD¹³ and CPCM solvent models for solution phase respectively yielded similar structures. We optimized the geometries from different starting points. In certain optimized structures, the intramolecular hydrogen-bonding was not observed, but since their energies were higher than the corresponding structures with H-bonds, they were not considered.

The initial structures of conjugate bases of the dimer was obtained by deleting the Hydrogen atom at the 1, 3 positions. After optimizing these structures, we arrive at a quite similar structures of the anion-1 and anion-3. This shows that, in an experimental system, the deprotonated site cannot be determined because the molecule will optimize itself to the intramolecular H-bonded structure which is not dependent on which of the differently positioned COOH group was deprotonated.

It should be noted that a slight variation in the structure gives very different values of energy.

An intramolecular hydrogen-bonding can be seen clearly for all anionic structures, leading to the molecule stabilization.

It is interesting to note that in figure 2c, the deprotonated carboxylic group is accepting two hydrogen bonds from the both sides. This leads to increased stabilization of this anionic structure as compared to those in figure 2b and 2d.

In all the anionic structures in figures 1, 2 and 3, it was observed that all the carboxylic

acids are participating in intramolecular H-bonding within the molecule. This leads to the formation of a helix-type structure if all the O are joined by an imaginary line. The same thing is not true for acid in which intramolecular H-bonding was not observed. It is also interesting to observe that the orientation of OH group in COOH is changed to anti when the group donates the Hydrogen to the COO⁻ group. This is because such orientation provides easier formation of H-bonds.

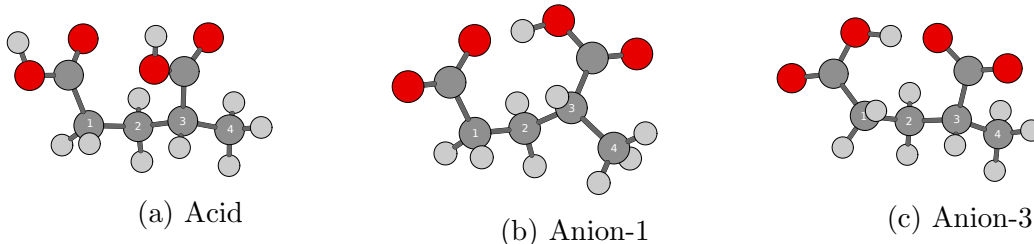


Figure 1: Optimized B3LYP/6-31G(2df,p) structure for Dimer of Acrylic acid and its possible conjugate bases. Color code: Red-Oxygen, Grey-Hydrogen, Black-Carbon.

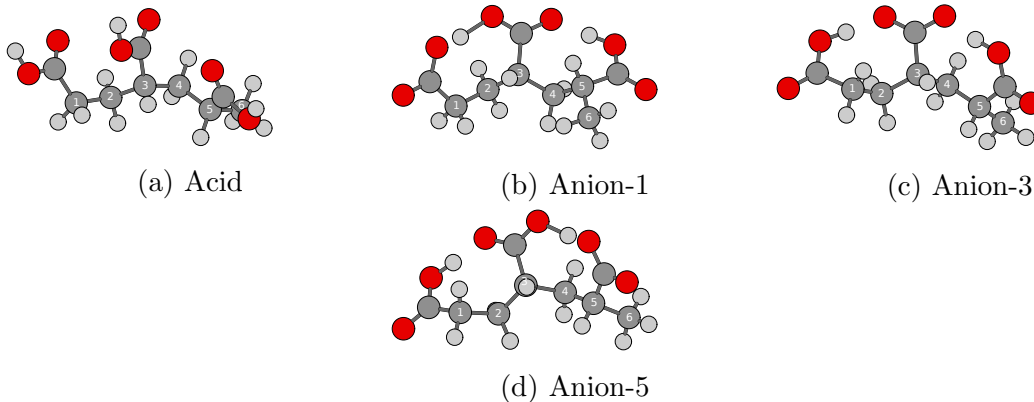


Figure 2: Optimized B3LYP/6-31G(2df,p) structure for Trimer of Acrylic acid and its possible conjugate bases. Color code: Red-Oxygen, Grey-Hydrogen, Black-Carbon.

In polymer physics, the Radius of gyration is used to approximate the dimension of a polymer chain. It is defined as the average distance of any atom from the center of mass of the polymer chain. The square of radius of gyration is defined as -

$$R_g^2 = \frac{1}{N} \sum_{k=1}^N (\vec{r}_k - \vec{r}_{cm})^2 \quad (6)$$

Where N is the number of atoms in the chain, \vec{r}_k is the position vector of the k^{th} atom, and \vec{r}_{cm} is the position vector of the center of mass of the chain which is given by -

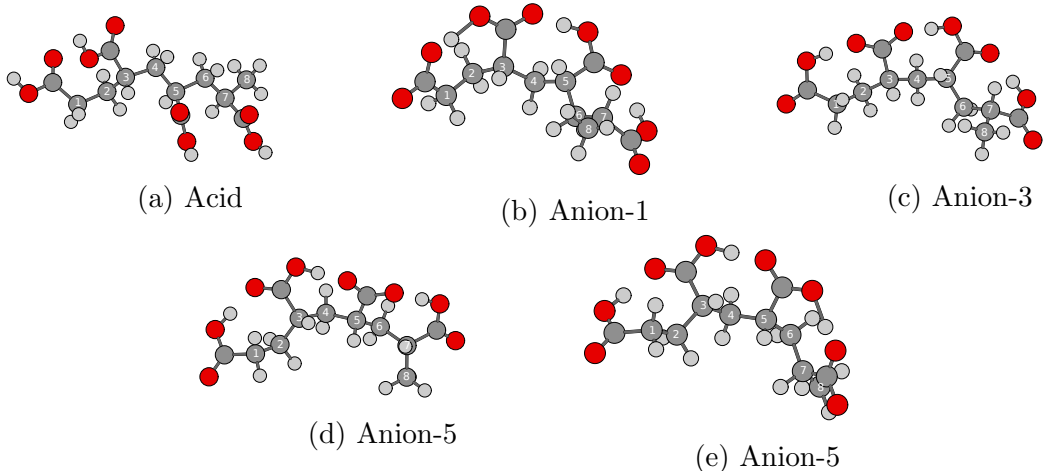


Figure 3: Optimized B3LYP/6-31G(2df,p) structure for Tetramer of Acrylic acid and its possible conjugate bases. Color code: Red-Oxygen, Grey-Hydrogen, Black-Carbon.

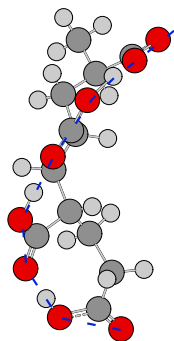


Figure 4: Optimized B3LYP/6-31G(2df,p) structure for anion-7. All the O atoms are on the path of a helix as shown by a dotted line.

$$\vec{r}_{cm} = \frac{1}{N} \sum_{k=1}^N \vec{r}_k \quad (7)$$

Radius of gyration has been computed by considering only the carbon atoms that forms the structure and neglecting the carbon from COOH groups. The values calculated using equation 6 has been reported in table 2. It can be concluded from the table 2 that R_g for each molecule is slightly less in presence of solvent field as compared to its gaseous optimized structure. This might not be true in case we take explicit solvents. This is because using implicit solvent fields, the H-bonding that may exist water and COO^- group which is not captured fully here.

Table 2: Radius of gyration (in Å) for each molecule was calculated using the Carbon atom of the structural frame.

Molecule	Single deprotonation		Molecule	Second deprotonation	
	Gas	SMD		Gas	SMD
Dimer (acid)	1.4974	1.4958	Dimer (Anion-1&3)	1.91075	1.91078
Dimer (Anion-1)	1.4971	1.4497	Trimer (Anion-1&3)	2.30965	2.27497
Dimer (Anion-3)	1.4972	1.8223	Trimer (Anion-3&5)	2.43704	2.39587
Trimer (Acid)	2.1851	2.2074	Trimer (Anion-5&1)	2.37316	2.30754
Trimer (Anion-1)	2.0863	2.0809	Tetramer (Anion-1&3)	2.47130	2.52291
Trimer (Anion-3)	2.1614	2.1562	Tetramer (Anion-1&5)	2.59831	2.55671
Trimer (Anion-5)	2.1615	2.1562	Tetramer (Anion-1&7)	2.60598	2.56137
Tetramer (Acid)	-	-	Tetramer (Anion-3&5)	2.71293	2.72355
Tetramer (Anion-1)	2.6647	2.6533	Tetramer (Anion-3&7)	2.72706	2.72653
Tetramer (Anion-3)	2.6903	2.6763	Tetramer (Anion-5&7)	2.55338	2.53800
Tetramer (Anion-5)	2.6890	2.6689	-	-	-
Tetramer (Anion-7)	2.7428	2.7279	-	-	-

Conclusion

Our theoretical calculations lack support from the experimental data. However, no direct experimental measurements are possible for the solvation free energies for a single ion.¹⁸ second source of uncertainty comes from the lack of experimental data for ions.

Although though our simulation, the optimized structures and therefore the energies of the conjugate bases for a particular molecule is different (depending on the position of COOH undergoing the deprotonation), in reality it might be true that the final optimized structure might not depend on the position. There is a possibility that all these structures might be interconvertible, each having a different probability of existing depending on its electronic energy values. This picture unfortunately could not be captured via the so-performed quantum mechanical optimization because each theory we have used in this study has its own limitations, and most of them are generally do not give best results when applied to larger molecules that were considered here.

Our study opens the scope for improvement of quantum mechanical methods to become computationally efficient and accurate for large molecules. This study is just a step forward in predicting the acidic properties of molecules with multiple acidic sites and their behavior at different degree of deprotonation.

References

1. Liptak, M. D.; Shields, G. C. Accurate pKa Calculations for Carboxylic Acids Using Complete Basis Set and Gaussian-n Models Combined with CPCM Continuum Solvation Methods. *Journal of the American Chemical Society* **2001**, *123*, 7314–7319, PMID: 11472159.
2. Sutton, C. C. R.; Franks, G. V.; da Silva, G. First Principles pKa Calculations on Carboxylic Acids Using the SMD Solvation Model: Effect of Thermodynamic Cycle, Model Chemistry, and Explicit Solvent Molecules. *The Journal of Physical Chemistry B* **2012**, *116*, 11999–12006, PMID: 22920269.
3. Lee, T. B.; McKee, M. L. Dependence of pKa on solute cavity for diprotic and triprotic acids. *Phys. Chem. Chem. Phys.* **2011**, *13*, 10258–10269.
4. Tummanapelli, A. K.; Vasudevan, S. Estimating successive pKa values of polyprotic acids from ab initio molecular dynamics using metadynamics: the dissociation of phthalic acid and its isomers. *Phys. Chem. Chem. Phys.* **2015**, *17*, 6383–6388.
5. Dong, H.; Du, H.; Qian, X. Theoretical Prediction of pKa Values for Methacrylic Acid Oligomers Using Combined Quantum Mechanical and Continuum Solvation Methods. *The Journal of Physical Chemistry A* **2008**, *112*, 12687–12694, PMID: 19053563.
6. Dong, H.; Du, H.; Qian, X. Theoretical Prediction of pKa Values for Methacrylic Acid Oligomers Using Combined Quantum Mechanical and Continuum Solvation Methods. *The Journal of Physical Chemistry A* **2008**, *112*, 12687–12694, PMID: 19053563.
7. Forsyth, W. R.; Antosiewicz, J. M.; Robertson, A. D. *Proteins-Struct. Funct. Genet.* **2002**, *48*, 388.
8. Liptak, M. D.; Shields, G. C. Experimentation with different thermodynamic cycles used for pKa calculations on carboxylic acids using complete basis set and Gaussiann models combined with CPCM continuum solvation methods. *International Journal of Quantum Chemistry* *85*, 727–741.
9. Tomasi, J.; Mennucci, B.; Cammi, R. Quantum Mechanical Continuum Solvation Models. *Chemical Reviews* **2005**, *105*, 2999–3094, PMID: 16092826.
10. Ho, J.; Coote, M. L. A universal approach for continuum solvent pK a calculations: are we there yet? *Theoretical Chemistry Accounts* **2009**, *125*, 3.

11. Ho, J.; Klamt, A.; Coote, M. L. Comment on the Correct Use of Continuum Solvent Models. *The Journal of Physical Chemistry A* **2010**, *114*, 13442–13444, PMID: 21133342.
12. Frisch, M. J.; Trucks, G. W.; Schlegel, H. B.; Scuseria, G. E.; Robb, M. A.; Cheeseman, J. R.; Scalmani, G.; Barone, V.; Mennucci, B.; Petersson, G. A. *et al.* Gaussian09 Revision E.01. Gaussian Inc. Wallingford CT 2009.
13. Marenich, A. V.; Cramer, C. J.; Truhlar, D. G. Universal Solvation Model Based on Solute Electron Density and on a Continuum Model of the Solvent Defined by the Bulk Dielectric Constant and Atomic Surface Tensions. *The Journal of Physical Chemistry B* **2009**, *113*, 6378–6396, PMID: 19366259.
14. Ochterski, J. W.; Petersson, G. A.; Jr., J. A. M. A complete basis set model chemistry. V. Extensions to six or more heavy atoms. *The Journal of Chemical Physics* **1996**, *104*, 2598–2619.
15. Pokon, E. K.; Liptak, M. D.; Feldgus, S.; Shields, G. C. Comparison of CBS-QB3, CBS-APNO, and G3 Predictions of Gas Phase Deprotonation Data. *The Journal of Physical Chemistry A* **2001**, *105*, 10483–10487.
16. Cossi, M.; Rega, N.; Scalmani, G.; Barone, V. Energies, structures, and electronic properties of molecules in solution with the CPCM solvation model. *Journal of Computational Chemistry* *24*, 669–681.
17. Sadlej-Sosnowska, N. Calculation of acidic dissociation constants in water: solvation free energy terms. Their accuracy and impact. *Theoretical Chemistry Accounts* **2007**, *118*, 281–293.
18. Dupont, C.; Andreussi, O.; Marzari, N. Self-consistent continuum solvation (SCCS): The case of charged systems. *The Journal of Chemical Physics* **2013**, *139*, 214110.